


**Magnetic control of heat generation in a magnetic tunnel contact with spin accumulation**

R. Jansen, A. Spiesser, and S. Yuasa

*Research Center for Emerging Computing Technologies, National Institute of Advanced Industrial Science and Technology (AIST), Tsukuba, Ibaraki 305-8568, Japan* (Received 27 June 2022; revised 11 September 2022; accepted 2 November 2022; published 23 November 2022)

It is described how the *heat* generation by an electrical current in a ferromagnetic tunnel contact to a nonmagnetic material depends on the spin accumulation in the nonmagnetic electrode for both Joule and Peltier heating. This enables the control of the heating in the tunnel contact by an external applied magnetic field that induces spin precession of the spin accumulation. Thereby, a Hanle type of spin signal is imprinted in the heating power. We derive expressions for the magnitude and sign of the magnetic-field-dependent heating power for Joule and Peltier heating, and discuss the important parameters. For contacts with small resistance-area product, the spin accumulation provides the dominant contribution to the Joule heating power, which can therefore be modulated by more than a factor of 2 with a magnetic field. The described phenomenon can also produce genuine spin signals in various devices, including nonlocal lateral spin valves.

DOI: [10.1103/PhysRevB.106.184421](https://doi.org/10.1103/PhysRevB.106.184421)**I. INTRODUCTION**

Since the start of spintronics research, a wide variety of electrical spin-transport phenomena have been discovered in magnetic materials and their nanostructures which have subsequently made their way into applications in magnetic recording and magnetic random access memory [1–4]. During the last decade, it has also become clear that in spintronic devices and systems, heat currents, and temperature gradients are ubiquitous and interact with spin currents and magnetization. Consequently, the field of spin caloritronics has flourished [5]. Following the exploration of the basic interplay between spin and heat [6–11], the more recent research activities can be divided into two main directions. The first is the investigation of the role of heat transport and temperature gradients in “conventional” spin-transport devices whose operation is based on purely electrical spin-transport principles. Since the electrical operation of those devices is inevitably accompanied by the generation of heat, the interactions between spin and heat may produce additional electrical spin signals and alter the overall device response. For instance, temperature gradients in nonlocal lateral spin valves can produce offset voltages in the nonlocal detection circuit [12–14], anisotropy of the nonlocal Hanle signals [15], and superimposed Hanle signals [16]. As another example, we mention spin pumping by ferromagnetic resonance in ferromagnet/nonmagnet bilayers. While it is known that the magnetization dynamics generates a spin current across the interface [17,18], it was shown recently that the heat generated by the resonant magnetization precession creates a temperature gradient that drives a separate and additional spin current [19,20]. The latter thus needs to be included in the analysis of spin-pumping experiments and can be used to increase the efficiency of spin-current generation [20]. The second recent direction in spin-caloritronics research involves the active control and manipulation of heat flow via the

interaction with the spin. Magnetic control of heat generation was observed in magnetoresistance devices, such as in magnetic metal spin-valve pillars [11], magnetic tunnel junctions [21], and magnetic multilayer nanowire networks [22], in which the generated heat depends on the relative magnetization alignment of the different ferromagnetic layers. Other examples of magnetic heat control, as recently reviewed by Uchida and Iguchi [23], include the modification of heat generation in ferromagnetic materials by magnetization direction, the manipulation of heat flow and thermal conductivity in magnetic nanostructures, and the active control of thermoelectric conversion by strain or electric fields.

Here we investigate heat generation in a basic ferromagnet/insulator/nonmagnet (FM/I/NM) tunnel structure that serves as a building block in spintronic devices, including nonlocal lateral spin valves, spin transistors, and spin-orbit torque tunnel devices. We shall examine theoretically how Joule and Peltier heating by an electrical current across such a tunnel contact depends on the spin accumulation in the nonmagnetic electrode. Since the spin accumulation can be manipulated by an external magnetic field that induces spin precession, the heat generation can be controlled by a magnetic field. We shall derive expressions for the magnitude and sign of the magnetic-field-dependent heating power for Joule and Peltier heating, and discuss the important parameters, notably, the resistance-area product of the tunnel contact. In addition, based on this quantitative analysis, we shall discuss recent experiments [16] on Hanle spin precession in Si-based nonlocal spin-transport devices, in which an additional contribution to the nonlocal Hanle spin signal that does not depend on the relative magnetization of injector and detector was observed, and for which it was proposed that this originates from the magnetic-field-dependent heat generation by the spin accumulation in the injector magnetic tunnel contact.

## II. RESULTS

In this section we derive expressions for the heating power in a FM/I/NM tunnel contact in which a spin accumulation exists in the nonmagnetic material. We shall consider a contact whose lateral dimensions are much larger than the spin-diffusion length in the nonmagnetic material, so that transport is essentially one dimensional. The magnitude of the spin accumulation right at the interface between the tunnel barrier and the nonmagnetic material is denoted by  $\Delta\mu$ . Inside the nonmagnetic electrode, the spin accumulation decays exponentially away from the tunnel interface. In principle, a spin accumulation is also induced in the ferromagnetic electrode. This is neglected because in ferromagnetic metals, spin relaxation is very fast so that the spin accumulation is negligibly small.

### A. Joule heating with a spin accumulation

In a linear transport description, the expressions [24] for the tunnel currents for majority ( $\uparrow$ ) and minority ( $\downarrow$ ) spin electrons are

$$I^\uparrow = G^\uparrow \left( V - \frac{\Delta\mu}{2e} \right), \quad (1)$$

$$I^\downarrow = G^\downarrow \left( V + \frac{\Delta\mu}{2e} \right), \quad (2)$$

with  $G^\uparrow$  and  $G^\downarrow$ , respectively, the tunnel conductance for majority and minority spin electrons,  $e$  the electronic charge, and  $V$  the bias voltage. Defining the total tunnel conductance as  $G = G^\uparrow + G^\downarrow$ , the spin polarization of the tunnel conductance as  $P_G = (G^\uparrow - G^\downarrow)/G$ , and the total current as  $I = I^\uparrow + I^\downarrow$ , we readily obtain  $V = I/G + P_G \Delta\mu/(2e)$ . Multiplying this by the total current  $I$ , and defining the tunnel resistance  $R_{\text{tun}} = 1/G$ , we obtain the Joule heating power  $P_{\text{Joule}}$  as

$$P_{\text{Joule}} = R_{\text{tun}} I^2 + P_G \left( \frac{\Delta\mu}{2e} \right) I. \quad (3)$$

The Joule heating power in a magnetic tunnel contact thus contains an extra term that depends directly on the magnitude of the spin accumulation. The extra term appears because the spin accumulation in the nonmagnetic electrode increases the voltage across the tunnel contact by an amount  $P_G \Delta\mu/(2e)$  at constant current.

If the tunnel resistance is large (i.e.,  $R_{\text{tun}} \gg r_s$ , with  $r_s$  the spin resistance [24,25] of the nonmagnetic material), the spin accumulation is small compared to the applied bias  $V$  and the spin current  $I_s$  that is injected into the nonmagnetic material is given by  $P_G I$ . In this regime, the spin-dependent part of the heating power is equal to the product of the spin current  $P_G I$  and the spin accumulation voltage  $\Delta\mu/(2e)$ . A simple microscopic picture then applies. Consider electrons that, after tunneling, move from the tunnel interface into the bulk of the nonmagnetic material, where the spin accumulation is reduced to zero. In doing so, the energy of the majority spin electrons, measured with respect to the majority spin electrochemical potential, *increases* by  $\Delta\mu/2$ . Via scattering the excess energy is released as heat, producing a heating power of  $(I^\uparrow/e)(\Delta\mu/2)$ . The minority spin electrons on average *lose* an energy of  $\Delta\mu/2$ , corresponding to a negative heating

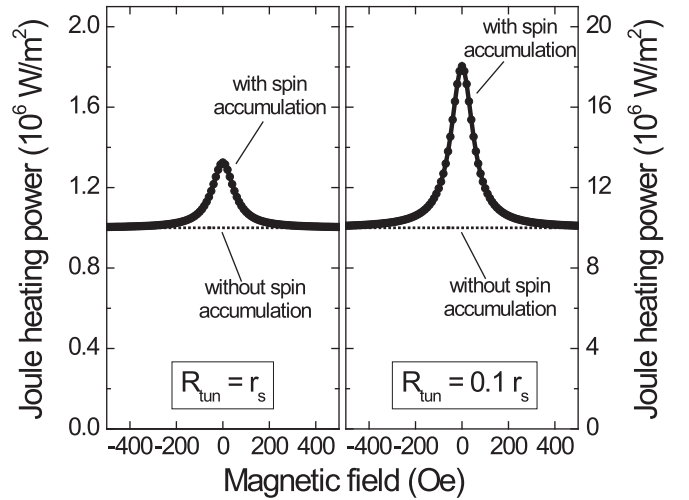


FIG. 1. Joule heating power of a FM/I/NM junction vs applied magnetic field perpendicular to the spin accumulation in the NM electrode for two different values of the tunnel resistance  $R_{\text{tun}}$  relative to the spin resistance  $r_s$  of the nonmagnetic material, as indicated. The spin-relaxation time was set to 1 ns. Other parameters are  $r_s = 100 \Omega \mu\text{m}^2$ ,  $P_G = 70\%$ . The tunnel current density was adjusted so as to obtain a tunnel bias voltage of 10 mV for both cases. A simple Lorentzian line shape was assumed.

power of  $-(I^\downarrow/e)(\Delta\mu/2)$ . The total heating power is then  $(I^\uparrow - I^\downarrow) \Delta\mu/(2e)$ , which indeed is the product of the spin current and the spin accumulation voltage. In Appendixes A and B we provide a more detailed derivation of Eq. (3) considering the energy dissipation per spin channel and discuss where the energy dissipation takes place.

The scaling of  $P_{\text{Joule}}$  with current is obtained by using the well-known expression for the spin accumulation,  $\Delta\mu/(2e) = P_G r_s^* I$ , in a one-dimensional transport description [24–26]. Here,  $r_s^*$  is the spin resistance  $r_s$  of the nonmagnetic material multiplied [27] by a factor  $R_{\text{tun}}/[R_{\text{tun}} + (1 - P_G^2) r_s]$  that takes into account that the spin accumulation has a back-effect on the injected spin current [24,25,28]. We then obtain

$$P_{\text{Joule}} = R_{\text{tun}} I^2 + P_G^2 r_s^* I^2. \quad (4)$$

The spin-dependent part of the Joule heating is thus quadratic in the current, as expected. Since  $P_G^2 r_s^*$  cannot be negative, the spin accumulation always enhances the Joule heating in the magnetic tunnel contact. Alternatively,  $P_{\text{Joule}}$  can be expressed in terms of  $\Delta\mu$  as

$$P_{\text{Joule}} = R_{\text{tun}} I^2 + \frac{1}{r_s^*} \left( \frac{\Delta\mu}{2e} \right)^2. \quad (5)$$

The notion that the Joule heating power has a contribution that is proportional to the spin accumulation implies that the Joule heating power is dependent on an external magnetic field. If it is perpendicular to the spins, the field induces spin precession and causes the spin accumulation to decay as a function of the magnetic field, which is known as the Hanle effect [1]. Although the Hanle effect is usually detected electrically, our analysis shows that a signature of the Hanle effect is also present in the Joule heating power, as illustrated in Fig. 1. Al-

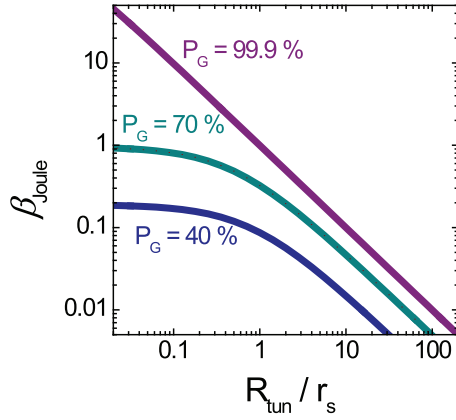


FIG. 2. Ratio  $\beta_{\text{Joule}}$ , defined as the spin-dependent part of the Joule heating power divided by the Joule heating power in the absence of spin accumulation, as a function of the tunnel resistance  $R_{\text{tun}}$  for three different values of the tunnel spin polarization  $P_G$ , as indicated.

though the precise dependence on the perpendicular magnetic field  $B_z$  is determined by the device geometry and parameters such as the spin-diffusion length, in its simplest form the Hanle line shape is Lorentzian with the spin accumulation decaying as  $1/(1 + \omega_z^2 \tau_s^2)$ , with  $\tau_s$  the spin-relaxation time in the nonmagnetic material, and  $\omega_z = \gamma B_z$  is the Larmor frequency ( $\gamma = g\mu_B/\hbar$  is the electron gyromagnetic ratio,  $\mu_B$  the Bohr magneton,  $g$  the electron  $g$  factor, and  $\hbar$  the reduced Planck's constant).

It is instructive to examine the ratio  $\beta_{\text{Joule}}$ , defined as the spin-dependent part of the Joule heating power divided by the Joule heating power in the absence of a spin accumulation. From Eq. (4) we obtain

$$\beta_{\text{Joule}} = \frac{P_G^2 r_s^*}{R_{\text{tun}}} = P_G^2 \left( \frac{r_s}{R_{\text{tun}} + (1 - P_G^2) r_s} \right). \quad (6)$$

For large tunnel resistance ( $R_{\text{tun}} \gg r_s$ ), the spin accumulation is small and yields a relatively small extra Joule heating power (although it is detectable, just as the charge voltage produced by the spin accumulation is detectable). As the tunnel resistance is reduced such that  $R_{\text{tun}} \leq r_s$ , the injected spin current and the spin accumulation become large, so that the spin-dependent part of the Joule heating becomes more important (Fig. 2). It can reach half of the total Joule heating power for  $P_G = 70\%$  ( $\beta_{\text{Joule}} \approx 1$ ). This implies that the presence of the spin accumulation enhances the Joule heating power by a factor of 2 compared to the heating power without spin accumulation. For half-metallic ferromagnets with  $P_G \approx 100\%$  and low-resistance tunnel contacts, the Joule heating power can be significantly enhanced and can even be dominated ( $\beta_{\text{Joule}} \gg 1$ ) by the spin-dependent part.

### B. Peltier heating with a spin accumulation

Next we examine how the spin accumulation contributes to the Peltier heat current through the tunnel contact. The Peltier heat currents  $I^{\mathcal{Q},\uparrow}$  and  $I^{\mathcal{Q},\downarrow}$  for each spin are given by [11,30]

$$I^{\mathcal{Q},\uparrow} = \Pi^\uparrow I^\uparrow = -L^\uparrow T_0 \left( V - \frac{\Delta\mu}{2e} \right), \quad (7)$$

$$I^{\mathcal{Q},\downarrow} = \Pi^\downarrow I^\downarrow = -L^\downarrow T_0 \left( V + \frac{\Delta\mu}{2e} \right), \quad (8)$$

with  $\Pi^\sigma = S^\sigma T_0$  the Peltier coefficient of the tunnel contact for each spin ( $\sigma = \uparrow, \downarrow$ ) at a temperature  $T_0$ , which is assumed to be independent of spin. The  $S^\sigma$  is the spin-dependent Seebeck coefficient, and  $L^\sigma = -S^\sigma G^\sigma$  is the thermoelectric conductance. The total heat current  $I^{\mathcal{Q}} = I^{\mathcal{Q},\uparrow} + I^{\mathcal{Q},\downarrow}$  through the tunnel region is then

$$I^{\mathcal{Q}} = -T_0 (L^\uparrow + L^\downarrow) V + T_0 (L^\uparrow - L^\downarrow) \left( \frac{\Delta\mu}{2e} \right). \quad (9)$$

Because for a constant current the voltage  $V$  depends on the spin accumulation, both terms in Eq. (9) depend on  $\Delta\mu$ . We eliminate  $V$  by inserting  $V = I/G + P_G \Delta\mu/(2e)$ , as obtained from Eqs. (1) and (2). After rewriting we then obtain

$$I^{\mathcal{Q}} = \Pi_0 I - \left( \frac{1 - P_G^2}{2R_{\text{tun}}} \right) (\Pi^\uparrow - \Pi^\downarrow) \left( \frac{\Delta\mu}{2e} \right). \quad (10)$$

Therefore the Peltier heat current has a contribution that is directly proportional to the spin accumulation, provided that the Peltier coefficient is spin dependent ( $\Pi^\uparrow \neq \Pi^\downarrow$ ). The Peltier coefficient  $\Pi_0$  in the absence of a spin accumulation is equal to  $S_0 T_0$ , with  $S_0 = -L/G$  the Seebeck coefficient in the absence of spin accumulation and  $L = L^\uparrow + L^\downarrow$ . Note that in the above description we have considered only the heat current carried by the tunneling electrons. In a FM/I/NM tunnel junction, the currents in the FM and NM leads are also accompanied by heat currents that need to be included [30]. Any difference in the heat currents between the FM and the NM electrode will produce heating or cooling (Peltier effect) at the tunnel interface; however, this does not affect the spin-dependent part of the heat current that originates from the spin accumulation.

By inserting  $\Delta\mu/(2e) = P_G r_s^* I$  we obtain

$$I^{\mathcal{Q}} = \Pi_0 I - P_G \left( \frac{1 - P_G^2}{2R_{\text{tun}}} \right) r_s^* (\Pi^\uparrow - \Pi^\downarrow) I. \quad (11)$$

The spin-dependent part of the Peltier heating is thus linear in the current, and the sign depends on the sign of the spin polarization of the Peltier coefficient. Also,  $\Pi_0$  and  $\Pi^\uparrow - \Pi^\downarrow$  do not necessarily have the same sign, so the spin accumulation may enhance or reduce the Peltier heat current through the tunnel contact. The ratio  $\beta_{\text{Peltier}}$ , defined as the spin-dependent part of the Peltier heat current divided by the Peltier heat current in the absence of a spin accumulation, is

$$\beta_{\text{Peltier}} = P_G \left( \frac{1 - P_G^2}{2} \right) \left( \frac{\Pi^\uparrow - \Pi^\downarrow}{\Pi_0} \right) \left( \frac{r_s}{R_{\text{tun}} + (1 - P_G^2) r_s} \right). \quad (12)$$

Just as for Joule heating, the spin-dependent part of the Peltier heat current depends on the ratio  $R_{\text{tun}}/r_s$  [Fig. 3(a)]. However, whereas  $\beta_{\text{Joule}}$  can reach values that are equal to or larger than unity,  $\beta_{\text{Peltier}}$  is generally much smaller than unity. Hence the spin accumulation has a relatively small effect on the Peltier heat current. Also note that the dependence on  $P_G$  is different [Fig. 3(b)]. The spin-dependent part of the Peltier

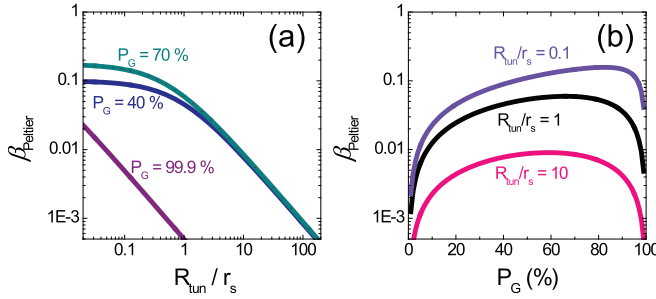


FIG. 3. (a) Ratio  $\beta_{\text{Peltier}}$ , defined as the spin-dependent part of the Peltier heat current divided by the Peltier heat current in the absence of spin accumulation, as a function of the tunnel resistance  $R_{\text{tun}}$  for three different values of the tunnel spin polarization  $P_G$ . The value of  $(\Pi^\uparrow - \Pi^\downarrow)/\Pi_0$  was set to  $+50\%$ . (b) Ratio  $\beta_{\text{Peltier}}$  as a function of  $P_G$  for three different values of  $R_{\text{tun}}$ , as indicated.

heat current increases with increasing  $P_G$ , but for very large values of  $P_G$ ,  $\beta_{\text{Peltier}}$  goes down and for purely half-metallic contacts with  $P_G = \pm 100\%$ , the spin-dependent part of the Peltier heat current vanishes. This, however, is a consequence of the linear dependence on the current and the assumption we made here that the (Hanle) measurement is done at a constant current. For instance, if  $P_G = +100\%$ , then  $I^{\downarrow} = 0$  and  $I^{\uparrow} = \Pi^\uparrow I^\uparrow = \Pi^\uparrow I$ , which is constant and independent of the spin accumulation if  $I$  is kept constant as the magnetic field is swept. If, on the other hand, the measurement is done at constant bias voltage  $V$ , the Peltier heat current would depend on the spin accumulation.

### C. Joule versus Peltier

We compare the heating produced by the spin accumulation for Joule and Peltier heating. We introduce the ratio  $\Gamma_{\text{Peltier}/\text{Joule}}$ , defined as the spin part of the Peltier heat current divided by the spin part of the Joule heating power, for a given value of  $\Delta\mu$ . We obtain

$$\Gamma_{\text{Peltier}/\text{Joule}} = -\left(\frac{1 - P_G^2}{2P_G}\right) \left(\frac{\Pi^\uparrow - \Pi^\downarrow}{R_{\text{tun}} I}\right). \quad (13)$$

Since the first term is of the order of unity for typical values of  $P_G$  in the 30%–70% range, the relative contribution of Joule and Peltier heating is determined by the ratio of the spin-dependent Peltier coefficient and the bias voltage  $R_{\text{tun}} I$  in the absence of a spin accumulation. The Seebeck coefficient of a tunnel contact can be around  $100 \mu\text{V}/\text{K}$ , so that for  $T_0 = 300 \text{ K}$ , the Peltier coefficients are of the order of several tens of millivolts. Since the tunnel bias is typically several hundred millivolts,  $\Gamma_{\text{Peltier}/\text{Joule}}$  is typically smaller than unity. The heat generated by the spin accumulation is thus dominated by the Joule heating, except for very small bias voltages below 10 mV (Fig. 4). However, note that for small tunnel spin polarizations (10% or less), the first term in Eq. (13) becomes large and the Peltier contribution dominates up to larger bias voltage. The relative sign of the two contributions depends on the sign of  $\Pi^\uparrow - \Pi^\downarrow$ , and so the two contributions can have equal or opposite signs.

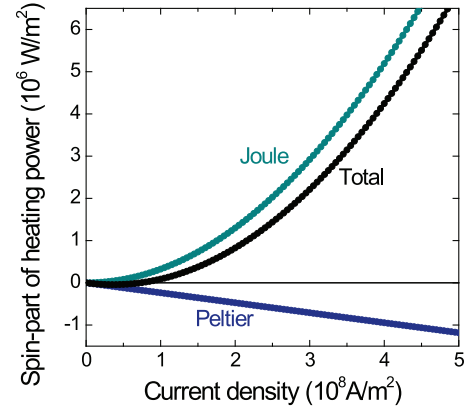


FIG. 4. Comparison of the spin-dependent part of the Joule heating power and the Peltier heat current as a function of the tunnel current density. The sum of the two contributions is also displayed. The parameters are  $P_G = 70\%$ ,  $R_{\text{tun}} = r_s = 100 \Omega \mu\text{m}^2$ ,  $\Pi^\uparrow = +30 \text{ mV}$ ,  $\Pi^\downarrow = +10 \text{ mV}$ .

### D. Beyond linear response: Nonlinear spin detection

The equations for the heating power were derived assuming linear transport. However, the largest heat currents are created at larger tunnel bias, for which nonlinear effects need to be taken into account. For the most part, this can be done by making all the parameters (such as  $P_G$ ,  $R_{\text{tun}}$ ,  $\Pi^\sigma$  etc.) dependent on the bias voltage. However, we need to take into account explicitly [31] the nonlinearity of the spin-detection efficiency  $P_{\text{det}}$ , which governs the conversion of the spin accumulation into a detectable charge voltage across the tunnel contact. In linear response  $P_{\text{det}} = P_G$ , but at larger bias this is no longer correct [31]. We therefore introduce a parameter  $\xi(V)$  that is defined as the ratio  $P_{\text{det}}/P_G$ . In linear response  $\xi(V) = 1$ , but at finite bias  $\xi(V)$  can be larger than unity, or much smaller, depending on the voltage across the tunnel contact [31]. The modified expressions for the charge currents are then

$$I^\uparrow = G^\uparrow \left[ V - \xi(V) \left( \frac{\Delta\mu}{2e} \right) \right] \quad (14)$$

$$I^\downarrow = G^\downarrow \left[ V + \xi(V) \left( \frac{\Delta\mu}{2e} \right) \right], \quad (15)$$

which leads to  $V = I/G + P_G \xi(V) \Delta\mu/(2e)$ . The extra voltage produced by the spin accumulation is thus proportional to  $P_G \xi(V) = P_{\text{det}}$ , instead of to  $P_G$ . The expression for the Joule heating power is then modified to

$$P_{\text{Joule}} = R_{\text{tun}} I^2 + P_G \xi(V) \left( \frac{\Delta\mu}{2e} \right) I, \quad (16)$$

and the Peltier heat current becomes

$$I^Q = \Pi_0 I - \left( \frac{1 - P_G^2}{2R_{\text{tun}}} \right) (\Pi^\uparrow - \Pi^\downarrow) \xi(V) \left( \frac{\Delta\mu}{2e} \right). \quad (17)$$

We thus find that the nonlinearity of spin detection not only modifies the charge voltage produced by the spin accumulation but also modifies the Joule and Peltier heating in the magnetic tunnel contact. The spin-detection efficiency at high bias can either be calculated (as previously done using a free-electron description of tunneling [31]) or it can be measured



[31] using a nonlocal device with a biased detector tunnel contact.

### III. DISCUSSION

The above analysis shows that the spin accumulation definitely contributes to the Joule and Peltier heating produced by a tunnel contact. Whereas for Peltier heating the spin accumulation plays a role only if the thermoelectric parameters (Peltier and Seebeck coefficient) are spin dependent [Eq. (10)], for Joule heating this is not required. We find that the Joule heating power can be significantly enhanced and can even be dominated by the contribution from the spin accumulation, provided that the resistance-area product of the contact is small ( $R_{\text{tun}} \leq r_s$ ) and the tunnel spin polarization is sufficiently large. Under these conditions, the Joule heating power can be modulated by more than a factor of 2 by a magnetic field. In the case of a single tunnel contact [32,33] considered here, the magnetic field needs to be applied perpendicular to the spins so as to induce spin precession, producing a Hanle type of response that typically has a Lorentzian line shape. Alternatively, a two-terminal device geometry [16,31,34–37] can be employed, with two ferromagnetic tunnel contacts on a nonmagnetic channel. The spin accumulation then depends on the relative magnetization alignment of the two contacts, and a spin-valve type of response will appear in the heating power.

For the detection of the modulation of the heating power by the spin accumulation one can use the different methods to detect spin-dependent thermoelectric effects described by Uchida *et al.* [23]. One can measure changes in the temperature in the relevant part of the device, for instance, using thermography with infrared radiation or thermoreflectance using the temperature dependence of optical reflection. Alternatively, one can convert the temperature gradients that result from the heating into an electrical voltage using the Seebeck effect, for instance, by attaching a thermocouple [23] or by measuring the Seebeck voltage across a detector junction in the device. Following the latter approach, we should expect that the dependence of the heating power on the spin accumulation can also produce genuine spin signals in spin-transport devices. For example, consider a nonlocal lateral spin-valve device. When a current is applied across the injector tunnel contact, a heat current is generated that depends on a magnetic field, as described above. The heat will spread through the channel of the device and is converted back into an electrical signal at the detector contact via the Seebeck effect. Because the heat current depends on the spin accumulation under the injector contact, a thermally mediated Hanle signal is produced in the nonlocal detection circuit. This signal will be added to the regular Hanle signal due to conventional electrical spin transport through the channel.

Let us discuss the expected sign and magnitude of such a thermally induced Hanle signal in a nonlocal device and compare it with recent experiments [16]. We start with the expected sign. The heat generated by the injector contact flows through the channel in both directions, producing lateral temperature gradients along the channel. The temperature at the position of the nonlocal magnetic detector contact will be higher than that of the nonmagnetic reference contact that is placed at the far end of the channel. Since

the Seebeck coefficient of an  $n$ -type Si channel is negative and  $\Delta V = -S\Delta T$ , the potential of the ferromagnetic detector is higher compared to that of the reference contact. Hence, the heat current produces a negative voltage in the nonlocal detector circuit for the wiring configuration used (plus terminal of the voltmeter on the reference contact, minus terminal on the FM detector contact [16]). As shown above, Joule heating is enhanced by the spin accumulation, which is largest at zero magnetic field. The expected signal thus consists of a negative offset voltage and a superimposed negative Hanle signal. The expected negative sign of the Hanle signal is consistent with what was observed in the recent experiments [16].

Next we examine the expected magnitude. The tunnel spin polarization of the contacts [16] is around 50% at 10 K, whereas  $R_{\text{tun}} = 27.6 \text{ k}\Omega \mu\text{m}^2$ . From the spin signal measured across the injector contact, we also obtain  $r_s = 0.8 \text{ k}\Omega \mu\text{m}^2$ , so that  $R_{\text{tun}}/r_s = 34.5$ . The expected ratio  $\beta_{\text{Joule}}$  is then 0.007. Thus only a very small fraction of the heat current is modulated by the spin accumulation. If we assume that the heat current creates a temperature difference in the nonlocal detector circuit of less than 10 K and we use a Seebeck coefficient of  $S = -40 \mu\text{V}/\text{K}$  for heavily doped  $n$ -type Si at low temperatures [38], the offset voltage produced would be  $-0.4 \text{ mV}$  at best. The Hanle signal would then be a small fraction of this, i.e.,  $-0.4 \text{ mV} \times 0.007 = -0.0028 \text{ mV}$  at best. However, a superimposed nonlocal Hanle signal with a magnitude of  $-0.36 \text{ mV}$  was observed [16]. In order to reconcile the experimental result with the theory developed here, one would either need a much larger temperature difference, which seems unlikely, or a larger Seebeck coefficient. If the Seebeck voltage arises across the detector tunnel junction rather than along the Si channel, then we should use the Seebeck coefficient of the tunnel contact. *Ab initio* calculations for epitaxial MgO-based magnetic metal tunnel junctions [39] yield values of  $S$  below  $100 \mu\text{V}/\text{K}$ . However, it has been shown that inelastic magnon excitations can significantly enhance the Seebeck coefficient of tunnel junctions [40,41]. Indeed, in some experiments Seebeck coefficients larger than  $1 \text{ mV}/\text{K}$  were reported for MgO-based magnetic metal tunnel contacts [42], while noting that the reliability of the extracted values depends on the reliability of the estimated temperature difference across the tunnel contact. Although it would seem that the superimposed nonlocal Hanle signals observed in Ref. [[16]] are larger than what we expect based on the theory presented here, for a definite answer one would need a precise determination of the temperature differences in the nonlocal detector circuit and an accurate value of the Seebeck coefficient of the detector tunnel contact.

In any case, our analysis shows that the modulation of Joule heating by the spin accumulation can produce Hanle signals in nonlocal devices and that significant signals appear when the  $R_{\text{tun}}$  is comparable to or smaller than  $r_s$ . In that case  $\beta_{\text{Joule}}$  is close to unity and the thermally induced nonlocal Hanle signal becomes comparable to the thermally induced nonlocal offset voltage. And for the latter, it is well known that it can be comparable to or even larger than the nonlocal spin signal produced by electrical spin transport [12–14]. Note that it is certainly possible to create magnetic tunnel contacts for which  $R_{\text{tun}}$  is comparable to  $r_s$ . For instance, in Ref. [[43]], the Si channel of the nonlocal devices had a spin resistance

$r_s$  of 2-3  $k\Omega \mu m^2$ , whereas the Fe/MgO tunnel contacts had a comparable resistance-area product at an MgO thickness around 0.9 nm. Unfortunately, whereas values of the tunnel spin polarization up to 90% are obtained at large MgO thickness [43],  $P_G$  was reduced to around 15% at 0.9 nm of MgO, and consequently, the value of  $\beta_{\text{Joule}}$  is only about 0.01 at  $R_{\text{tun}} \approx r_s$ . One would thus require a larger  $P_G$  at small MgO thickness to enhance the effects described here. Interestingly, under the conditions for obtaining large magnetoresistance in a two-terminal device [25] ( $R_{\text{tun}} \approx r_s$  and large  $P_G$ ), the thermal effects described here will also be enhanced and come into play.

#### IV. SUMMARY

We have theoretically examined how the heat generation by an electrical current in a ferromagnetic tunnel contact to a nonmagnetic material depends on the spin accumulation in the nonmagnetic electrode. We derived expressions for the magnitude and the sign of the contribution of the spin accumulation to the heating power for Joule and Peltier heating, and discussed the important parameters. For contacts with small resistance-area product, the spin accumulation provides a significant contribution to the Joule heating power, which can therefore be modulated by more than a factor of 2 with a magnetic field that induces spin precession of the spin accumulation. Thereby, a Hanle spin signal is imprinted in the heating power. The influence of the spin accumulation on the Peltier heat current is generally smaller. The described phenomenon enables magnetic control of heat generation, but it can also produce genuine spin signals in various spin-transport devices, including nonlocal lateral spin valves. Our analysis, however, reveals that in general significant thermally mediated Hanle spin signals are to be expected only when the resistance-area product of the tunnel contact is small.

#### APPENDIX A

In this Appendix we discuss the effect of the spin accumulation on the Joule heating power in more detail, paying particular attention to where the energy dissipation occurs. We compare the Joule heating power calculated by considering the tunnel contact as a “black box resistor” with current  $I$  and voltage  $V$ , with the result obtained by calculating the heating power for each spin channel and then adding this up.

We consider a tunnel contact (Fig. 5) in which tunneling is purely elastic. This implies that no energy dissipation occurs within the tunnel barrier itself. Therefore when calculating the Joule heating power of a (nonmagnetic) tunnel contact, one normally considers that the tunneling electrons, which enter the nonmagnetic electrode with excess energy  $eV$ , thermalize within a very short distance from the tunnel interface. The energy dissipation thus occurs on the length scale  $\xi_{th}$  of the thermalization. Energy relaxation in nonmagnetic materials is much faster than spin relaxation, so  $\xi_{th}$  is very small compared to the spin-diffusion length  $L_{SD}$ . Therefore, within a length of  $\xi_{th}$  from the tunnel interface, the spin-dependent electrochemical potentials are considered to be constant and equal to their values right at the tunnel interface where the spin accumulation is maximal. Majority and minority spin electrons then enter the nonmagnetic material with different

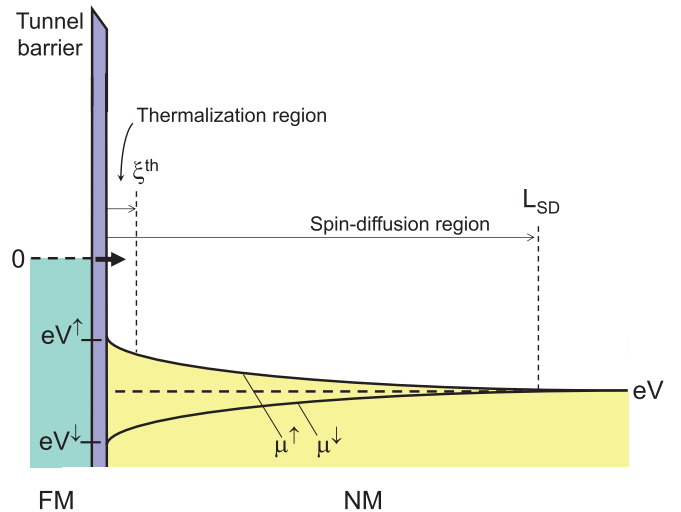


FIG. 5. Schematic energy-band diagram of a tunnel contact between a ferromagnet (FM) and a nonmagnetic material (NM) with a spin accumulation characterized by spin-dependent electrochemical potentials  $\mu^\uparrow$  and  $\mu^\downarrow$  that decay exponentially with distance from the tunnel interface. The regions where thermalization and spin diffusion of the injected electrons occur are indicated. Note that  $\xi_{th} \ll L_{SD}$ , and that the horizontal and vertical axes are not to scale.

excess energy  $eV^\uparrow$  and  $eV^\downarrow$  with  $V^{\uparrow,\downarrow} = V \mp \Delta\mu/(2e)$ . Following this approach, the Joule heating power  $P_{\text{Joule}}^{th}$  associated with the thermalization region is obtained by adding up the dissipation for the two spin channels, which yields

$$P_{\text{Joule}}^{th} = I^\uparrow V^\uparrow + I^\downarrow V^\downarrow = (I^\uparrow + I^\downarrow) V - (I^\uparrow - I^\downarrow) \left( \frac{\Delta\mu}{2e} \right). \quad (\text{A1})$$

By inserting the expressions (1) and (2) for  $I^\sigma$  we obtain

$$P_{\text{Joule}}^{th} = R_{\text{tun}} I^2 + P_G I \left( \frac{\Delta\mu}{2e} \right) - I_s \left( \frac{\Delta\mu}{2e} \right). \quad (\text{A2})$$

The first two terms on the right-hand side correspond to the result given for the Joule heating power in the main text, Eq. (3). It is what one would obtain if one considers the contact as a “black box resistor.” The third term on the right-hand side is proportional to the spin current  $I_s = I^\uparrow - I^\downarrow$ , which is given by

$$I_s = P_G I - G(1 - P_G^2) \left( \frac{\Delta\mu}{2e} \right). \quad (\text{A3})$$

The spin current is equal to  $P_G I$  minus a correction that becomes important for large  $\Delta\mu$ , i.e., when the tunnel resistance becomes comparable to or smaller than  $r_s$ . If the tunnel resistance is large ( $R_{\text{tun}} \gg r_s$ ) and the spin current is equal to  $P_G I$ , the last two terms on the right-hand side of Eq. (A2) cancel out and  $P_{\text{Joule}}^{th}$  becomes equal to  $R_{\text{tun}} I^2$ , which is independent of the spin accumulation. Thus if we consider only the energy dissipation within a thermalization length from the interface, the spin accumulation has no ( $R_{\text{tun}} \gg r_s$ ) or very little effect ( $R_{\text{tun}} \leq r_s$ ) on the Joule heating power.

However, it is essential to realize that there is an additional source of Joule heating. Additional energy dissipation is produced on the scale of the spin-diffusion length, because the

TABLE I. Spin-dependent and regular spin-independent contributions to the Joule heating power in a tunnel contact with spin accumulation.

	$R_{\text{tun}} \gg r_s$		$R_{\text{tun}} \leq r_s$	
	Regular Joule heating	Spin-dependent Joule heating	Regular Joule heating	Spin-dependent Joule heating
Thermalization region (length scale $\xi_{th}$ )	$R_{\text{tun}} I^2$	Negligible	$R_{\text{tun}} I^2$	$G(1 - P_G^2)(\frac{\Delta\mu}{2e})^2$
Spin-diffusion region (length scale $L_{SD}$ )	-	$P_G I(\frac{\Delta\mu}{2e})$	-	$P_G I(\frac{\Delta\mu}{2e}) - G(1 - P_G^2)(\frac{\Delta\mu}{2e})^2$

spin accumulation decays exponentially away from the tunnel interface and thus the spin-dependent electrochemical potentials are not constant up to a distance of the order of  $L_{SD} \gg \xi_{th}$  from the interface. As explained in the main text just below Eq. (3), the associated Joule heating  $P_{\text{Joule}}^{\text{acc}}$  in the region in which the spin accumulation exists is equal to the product of the injected spin current  $I_s$  and the spin accumulation voltage  $\Delta\mu/(2e)$ . Consider electrons that, after thermalization, move into the bulk of the nonmagnetic material, where the spin accumulation is reduced to zero. In doing so, the energy of the majority spin electrons, measured with respect to the majority spin electrochemical potential, *increases* by  $\Delta\mu/2$ . Via scattering the excess energy is released as heat, producing a heating power of  $(I^\uparrow/e)(\Delta\mu/2)$ . Similarly, the minority spin electrons on average *lose* an energy of  $\Delta\mu/2$ , corresponding to a negative heating power of  $-(I^\downarrow/e)(\Delta\mu/2)$ . The heating power associated with the spin accumulation region is then

$$P_{\text{Joule}}^{\text{acc}} = (I^\uparrow - I^\downarrow) \left( \frac{\Delta\mu}{2e} \right). \quad (\text{A4})$$

Adding this to  $P_{\text{Joule}}^{\text{th}}$  yields for the total Joule heating power

$$P_{\text{Joule}} = R_{\text{tun}} I^2 + P_G I \left( \frac{\Delta\mu}{2e} \right), \quad (\text{A5})$$

which is the result given in the main text, Eq. (3). We conclude that the Joule heating power can be obtained by calculating the heating power for each spin channel and adding these up, but care has to be taken to include the energy dissipation in the entire region in which the spin accumulation exists (length scale  $L_{SD}$ ). In fact, the latter dominates the spin-dependent part of the Joule heating power, whereas the Joule heating power associated with the thermalization (length scale  $\xi_{th}$ ) contributes very little to the spin dependence unless  $R_{\text{tun}} \leq r_s$ . This is summarized in Table I.

## APPENDIX B

In this Appendix we consider selected device structures and briefly discuss in what area of the device the spin-dependent part of the Joule heating is generated. For simplicity, we consider the regime with  $R_{\text{tun}} \gg r_s$ , so that the dissipation associated with the spin-dependent part of the Joule heating occurs in the area of the device where the spin accumulation decays (see Appendix A). The area of dissipation is schematically illustrated in Fig. 6. For a FM contact having a width  $W \gg L_{SD}$  and a thick NM channel with

a thickness  $t_{ch} \gg L_{SD}$ , the spin accumulation mainly decays into the depth direction away from the interface, and the dissipation associated with the spin-dependent part of the Joule heating occurs up to a depth of the order of  $L_{SD}$  [Fig. 6(a)]. However, for a thin NM channel having  $t_{ch} \ll L_{SD}$ , the spin accumulation is essentially constant into the depth direction and the decay of the spin accumulation occurs laterally along the channel. For a thin channel with a wide contact  $W \gg L_{SD}$  [Fig. 6(b)], the spin accumulation is constant in the central region under the contact [44], and the decay occurs near the edges of the FM contact within a spin-diffusion length. The dissipation associated with the spin-dependent part of the Joule heating thus occurs near the edges of the contact. For

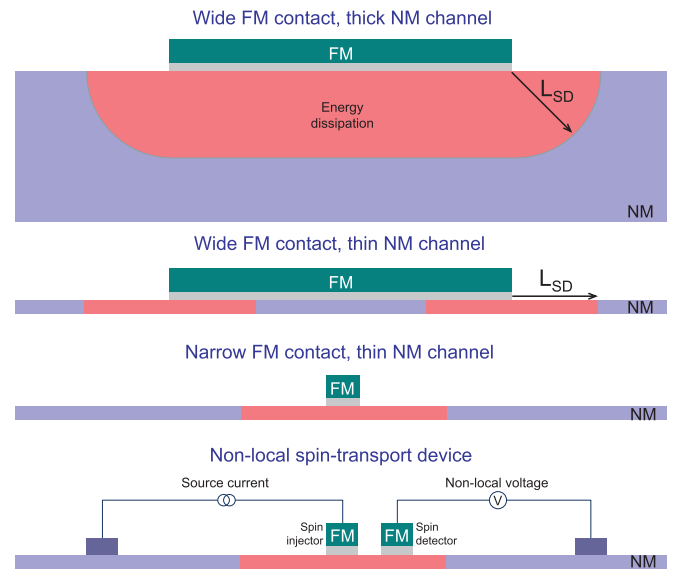


FIG. 6. Schematic illustration of selected device geometries for a FM tunnel contact on a NM channel, with the red colored areas indicating where the dissipation associated with the spin-dependent part of the Joule heating occurs, for (a) a wide FM contact ( $W \gg L_{SD}$ ) on a thick NM channel ( $t_{ch} \geq L_{SD}$ ), (b) a wide FM contact ( $W \gg L_{SD}$ ) on a thin NM channel ( $t_{ch} \ll L_{SD}$ ), (c) a narrow contact ( $W \leq L_{SD}$ ) on a thin NM channel ( $t_{ch} \ll L_{SD}$ ), and (d) a nonlocal device with a thin NM channel and FM injector and detector contacts of width  $\leq L_{SD}$ . Note that we have used the color only to indicate *where* the dissipation occurs, but we did not use a color scale to indicate the amount of dissipation, even though the dissipation depends on position in the NM channel and is different for each device geometry.

a thin channel with a narrow contact  $W \leq L_{SD}$  [Fig. 6(c)] the decay of the spin accumulation is also in the lateral direction, but it starts from the center of the contact [44], and so does the associated dissipation. Finally, the decay is similar for a nonlocal device [Fig. 6(d)] in which typically  $t_{ch} \ll L_{SD}$  and

$W \leq L_{SD}$ . Since the FM detector contact is placed within a spin-diffusion length from the FM injector contact, the region of dissipation associated with the spin-dependent part of the Joule heating extends to under the detector contact and beyond.

- 
- [1] I. Žutić, J. Fabian, and S. Das Sarma, Spintronics: Fundamentals and applications, *Rev. Mod. Phys.* **76**, 323 (2004).
- [2] A. Fert, Nobel lecture: Origin, development, and future of spintronics, *Rev. Mod. Phys.* **80**, 1517 (2008).
- [3] S. Sugahara and J. Nitta, Spin-transistor electronics: An overview and outlook, *Proc. IEEE* **98**, 2124 (2010).
- [4] R. Jansen, Silicon spintronics, *Nat. Mater.* **11**, 400 (2012).
- [5] G. E. W. Bauer, E. Saitoh, and B. J. van Wees, Spin caloritronics, *Nat. Mater.* **11**, 391 (2012).
- [6] M. Johnson and R. H. Silsbee, Thermodynamic analysis of interfacial transport and of the thermomagnetolectric system, *Phys. Rev. B* **35**, 4959 (1987).
- [7] K. Uchida, S. Takahashi, K. Harii, J. Ieda, W. Koshibae, K. Ando, S. Maekawa, and E. Saitoh, Observation of the spin Seebeck effect, *Nature (London)* **455**, 778 (2008).
- [8] A. Slachter, F. L. Bakker, J. P. Adam, and B. J. van Wees, Thermally driven spin injection from a ferromagnet into a nonmagnetic metal, *Nat. Phys.* **6**, 879 (2010).
- [9] J.-C. Le Breton, S. Sharma, H. Saito, S. Yuasa, and R. Jansen, Thermal spin current from a ferromagnet to silicon by Seebeck spin tunnelling, *Nature (London)* **475**, 82 (2011).
- [10] M. Walter, J. Walowski, V. Zbarsky, M. Münzenberg, M. Schäfers, D. Ebke, G. Reiss, A. Thomas, P. Peretzki, M. Seibt, J. S. Moodera, M. Czerner, M. Bachmann, and C. Heiliger, Seebeck effect in magnetic tunnel junctions, *Nat. Mater.* **10**, 742 (2011).
- [11] J. Flipse, F. L. Bakker, A. Slachter, F. K. Dejene, and B. J. van Wees, Direct observation of the spin-dependent Peltier effect, *Nat. Nanotechnol.* **7**, 166 (2012).
- [12] F. Casanova, A. Sharoni, M. Erekhinsky, and I. K. Schuller, Control of spin injection by direct current in lateral spin valves, *Phys. Rev. B* **79**, 184415 (2009).
- [13] F. L. Bakker, A. Slachter, J.-P. Adam and B. J. van Wees, Interplay of Peltier and Seebeck Effects in Nanoscale Nonlocal Spin Valves, *Phys. Rev. Lett.* **105**, 136601 (2010).
- [14] S. Kasai, S. Hirayama, Y. K. Takahashi, S. Mitani, K. Hono, H. Adachi, J. Ieda, and S. Maekawa, Thermal engineering of non-local resistance in lateral spin valves, *Appl. Phys. Lett.* **104**, 162410 (2014).
- [15] K. S. Das, F. K. Dejene, B. J. van Wees, and I. J. Vera-Marun, Anisotropic Hanle line shape via magnetothermoelectric phenomena, *Phys. Rev. B* **94**, 180403(R) (2016).
- [16] R. Jansen, A. Spiesser, Y. Fujita, H. Saito, S. Yamada, K. Hamaya, and S. Yuasa, Superimposed contributions to two-terminal and nonlocal spin signals in lateral spin-transport devices, *Phys. Rev. B* **104**, 144419 (2021).
- [17] Y. Tserkovnyak, A. Brataas, and G. E. W. Bauer, Enhanced Gilbert Damping in Thin Ferromagnetic Films, *Phys. Rev. Lett.* **88**, 117601 (2002).
- [18] K. Ando, Dynamical generation of spin currents, *Semicond. Sci. Technol.* **29**, 043002 (2014).
- [19] K. Yamanoi, Y. Yokotani, and T. Kimura, Dynamical Spin Injection Based on Heating Effect due to Ferromagnetic Resonance, *Phys. Rev. Appl.* **8**, 054031 (2017).
- [20] S. Obinata, R. Iimori, K. Ohnishi, and T. Kimura, Influence of heat flow control on dynamical spin injection in CoFeB/Pt/CoFeB trilayer, *Sci. Rep.* **12**, 3467 (2022).
- [21] J. Shan, F. K. Dejene, J. C. Leutenantsmeyer, J. Flipse, M. Münzenberg, and B. J. van Wees, Comparison of the magneto-Peltier and magneto-Seebeck effects in magnetic tunnel junctions, *Phys. Rev. B* **92**, 020414(R) (2015).
- [22] T. da Câmara Santa Clara Gomes, F. Abreu Araujo, and Luc Piraux, Making flexible spin caloritronic devices with interconnected nanowire networks, *Sci. Adv.* **5**, eaav2782 (2019).
- [23] K. Uchida and R. Iguchi, Spintronic thermal management, *J. Phys. Soc. Jpn.* **90**, 122001 (2021).
- [24] R. Jansen, S. P. Dash, S. Sharma, and B. C. Min, Silicon spintronics with ferromagnetic tunnel devices, *Semicond. Sci. Technol.* **27**, 083001 (2012).
- [25] A. Fert and H. Jaffrès, Conditions for efficient spin injection from a ferromagnetic metal into a semiconductor, *Phys. Rev. B* **64**, 184420 (2001).
- [26] The relation between  $\Delta\mu$  and  $I$  is different when the lateral dimension of the tunnel contact is comparable to or smaller than the spin-diffusion length and lateral spin diffusion away from the contact needs to be taken into account [24]. Moreover, corrections are needed when the thickness of the NM electrode is smaller than the spin-diffusion length [24]. Whereas this affects the magnitude of  $\Delta\mu$  for a given current, the relation between the  $P_{\text{Joule}}$  and  $\Delta\mu$  is still given by Eq. (3).
- [27] The spin resistance  $r_s$  is usually given in units of  $\Omega \text{ m}^2$ . Depending on whether one uses current or current densities,  $R_{\text{tun}}$  and/or  $r_s^*$  should be multiplied/divided by the tunnel contact area so as to obtain the same units for both terms in the heating power.
- [28] We assume that the tunnel resistance  $R_{\text{tun}}$  is always larger than the spin resistance of the ferromagnetic electrode. This is appropriate for tunnel contacts or for direct contacts between a ferromagnetic metal and a nonmagnetic semiconductor. However, for direct contacts of a ferromagnetic metal on a nonmagnetic metal, the interface resistance may be smaller than the spin resistance of the ferromagnetic electrode, and the conductivity mismatch [29] needs to be taken into account.
- [29] G. Schmidt, D. Ferrand, L. W. Molenkamp, A. T. Filip, and B. J. van Wees, Fundamental obstacle for electrical spin injection from a ferromagnetic metal into a diffusive semiconductor, *Phys. Rev. B* **62**, R4790 (2000).
- [30] B. Scharf, A. Matos-Abiague, I. Žutić, and J. Fabian, Theory of thermal spin-charge coupling in electronic systems, *Phys. Rev. B* **85**, 085208 (2012).



- [31] R. Jansen, A. Spiesser, H. Saito, Y. Fujita, S. Yamada, K. Hamaya, and S. Yuasa, Nonlinear Electrical Spin Conversion in a Biased Ferromagnetic Tunnel Contact, *Phys. Rev. Appl.* **10**, 064050 (2018).
- [32] X. Lou, C. Adelman, M. Furis, S. A. Crooker, C. J. Palmström, and P. A. Crowell, Electrical Detection of Spin Accumulation at a Ferromagnet-Semiconductor Interface, *Phys. Rev. Lett.* **96**, 176603 (2006).
- [33] S. P. Dash, S. Sharma, R. S. Patel, M. P. de Jong, and R. Jansen, Electrical creation of spin polarization in silicon at room temperature, *Nature (London)* **462**, 491 (2009).
- [34] T. Sasaki, T. Suzuki, Y. Ando, H. Koike, T. Oikawa, Y. Suzuki, and M. Shiraishi, Local magnetoresistance in Fe/MgO/Si lateral spin valve at room temperature, *Appl. Phys. Lett.* **104**, 052404 (2014).
- [35] M. Gurrum, S. Omar, and B. J. van Wees, Bias induced up to 100% spin-injection and detection polarizations in ferromagnet/bilayer-hBN/graphene/hBN heterostructures, *Nat. Commun.* **8**, 248 (2017).
- [36] M. Oltcher, F. Eberle, T. Kuczmiak, A. Bayer, D. Schuh, D. Bougeard, M. Ciorga, and D. Weiss, Gate-tunable large magnetoresistance in an all-semiconductor spin valve device, *Nat. Commun.* **8**, 1807 (2017).
- [37] A. Spiesser, Y. Fujita, H. Saito, S. Yamada, K. Hamaya, S. Yuasa, and R. Jansen, Hanle spin precession in a two-terminal lateral spin valve, *Appl. Phys. Lett.* **114**, 242401 (2019).
- [38] L. Weber and E. Gmelin, Transport properties of silicon, *Appl. Phys. A* **53**, 136 (1991).
- [39] C. Heiliger, C. Franz, and M. Czerner, *Ab initio* studies of the tunneling magneto-Seebeck effect: Influence of magnetic material, *Phys. Rev. B* **87**, 224412 (2013).
- [40] E. McCann and V. I. Fal'ko, Giant magnetothermopower of magnon-assisted transport in ferromagnetic tunnel junctions, *Phys. Rev. B* **66**, 134424 (2002).
- [41] E. McCann and V. I. Fal'ko, A tunnel junction between a ferromagnet and a normal metal: Magnon-assisted contribution to thermopower and conductance, *J. Magn. Magn. Mater.* **268**, 123 (2004).
- [42] A. Boehnke, U. Martens, C. Sterwerf, A. Niesen, T. Huebner, M. von der Ehe, M. Meinert, T. Kuschel, A. Thomas, C. Heiliger, M. Münzenberg, and G. Reiss, Large magneto-Seebeck effect in magnetic tunnel junctions with half-metallic Heusler electrodes, *Nat. Commun.* **8**, 1626 (2017).
- [43] A. Spiesser, H. Saito, S. Yuasa, and R. Jansen, Tunnel spin polarization of Fe/MgO/Si contacts reaching 90% with increasing MgO thickness, *Phys. Rev. B* **99**, 224427 (2019).
- [44] A. Spiesser, H. Saito, Y. Fujita, S. Yamada, K. Hamaya, S. Yuasa, and R. Jansen, Giant Spin Accumulation in Silicon Nonlocal Spin-Transport Devices, *Phys. Rev. Appl.* **8**, 064023 (2017).